384Gb/s PAM Transmission with CMOS-class Driving Voltage, Optical&RF-amplifier-free Reception and Low-complexity DSP Using a High-slope-efficiency Modulator

Paikun Zhu(1), Yuya Yamaguchi(1), Yuki Yoshida(1), Pham Tien Dat(1), Masayuki Motoya(2), Shingo Takano(2), Ryo Shimizu(2), Ken-ichi Kitayama(1)(3) and Kouichi Akahane(1)

(1) National Institute of Information and Communications Technology (NICT), Tokyo, Japan
{pkzhu3 , yamaguchi , yuki}@nict.go.jp
(2) Sumitomo Osaka Cement Company, Ltd., Chiba, Japan
(3) Hamamatsu Photonics Central Research Laboratory, Hamamatsu, Japan

Abstract *Using a high-slope-efficiency broadband modulator with theoretically-predicted merit, we demonstrated 900mV$_{pp}$-driving, 384Gb/s PAM8 over 300m SMF in C-band with no Tx DSP, Rx-side symbol-spaced 41-feedforward & 1-feedback-tap DFE, and hard-decision FEC. No optical or RF amplification was used for reception.*

Introduction

Short-reach intensity-modulation direct-detection (IM-DD) systems with high data rate, e.g., beyond 300Gb/s, have potential applications of low-lane-count datacenter interconnects (DCI) [1], future business local area networks [2] and so forth. Despite the data rate, the system should be designed to be simpler than high-speed core/metro ones. At analog side, operating with CMOS-class driving voltages (e.g., sub-1V$_{pp}$ [3]) is an attractive goal for a power-efficient transmitter (Tx); omitting optical and radio-frequency (RF) amplifiers at the receiver would be laudable as well. At digital side, N-ary pulse amplitude modulation (PAM-*N*) format may be preferred over more complex modulation like DMT to save one high-resolution digital-to-analog converter (DAC), while the capacity can still be appealing. Also, the receiver- (Rx-) side digital signal processing (DSP) should be complexity-bounded and implementation-friendly.

An electro-optical modulation device is one of the key components for short-reach links. For systems using external modulation, e.g., via a Mach-Zehnder modulator (MZM), recently remarkable progress has been made on increasing the 3dB bandwidth (BW) for high-data-rate transmission. Several materials/platforms were explored, such as Lithium Niobate (LN) [4], silicon photonics (SiPh) [5], plasmonics [6] and hybrid ones [7]. However, in most >300Gb/s demonstrations, optical and/or RF amplifiers were needed to compensate for the RF-to-RF signal loss during E/O (& O/E) conversion; moreover, Tx & Rx DSP were still relatively complicated regarding industry's range of interest (e.g., no Tx DSP; Rx equalizer has ~30 feedforward (FF) and 0~2 feedback (FB) taps [8, 9]).

In this work, we report fully-optical&RF-amplifier-free reception of 384Gb/s PAM8 signal transmission with low DSP complexity simultaneously. A prototype LN MZM was incorporated, designed with high figure of merit (FoM) "slope efficiency (SLE)" that directly reveals the RF-to-RF signal loss and takes into account not only 3dB BW but also half-wave voltage V$_\pi$ and optical losses of modulators. Theoretical analysis and results reveal that system performance can be competitive with the high-SLE MZM even if the 3dB bandwidth seems not advantageous. Experiments demonstrate that **(1)** only 900mV$_{pp}$ driving voltage was needed; **(2)** no optical or RF amplification was used for reception; **(3)** No Tx DSP (pre-emphasis, spectral shaping, etc.) was used while Rx-side equalizer was a symbol-spaced decision-feedback equalizer (DFE) with only 41 FF and 1 FB taps considering 20% hard-decision forward-error correction (HD-FEC).

SLE model and theoretical system symbol/bit error rate (SER/BER)

The frequency-dependent SLE of a traveling-

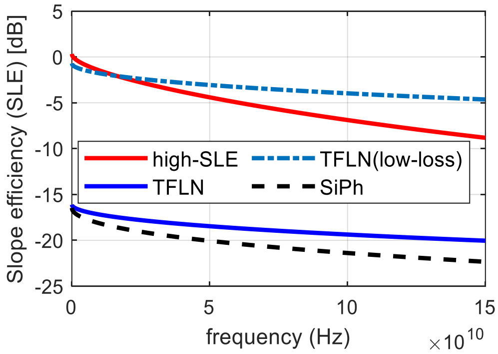

Fig. 1. Theoretical link gain (in dB) of our high-SLE MZM, a TFLN MZM and a silicon photonic (SiPh) MZM.

wave MZM s_{MZM} is defined as [10]

$$s_{MZM}(f) = \frac{\pi}{2}\frac{P_{LD}RT_{ff}}{V_\pi(f)} \qquad (1)$$

Where P_{LD}, R, V_π and T_{ff} denote laser power, source impedance, half-wave voltage and fiber-to-chip-to-fiber transmittance (inverse of coupling loss l_C times propagation loss l_P) respectively. The *RF-to-RF signal gain/loss G(f)* of an IM-DD link, or the power ratio of an RF input and the corresponding output, is [10]

$$G(f) = s^2_{mod}(f) r^2_{PD}(f) \qquad (2)$$

Where r_{PD} is the responsivity of the photodetector (PD). In essence, higher G means a less-lossy electro-optical link, indicating less demand for optical/RF amplifiers and being helpful to operate with CMOS-class voltage like sub-1V. Here, we focus on the impact of modulator and assume the PD is ideal (e.g., r_{PD} is unity (A/W)). In this case, SLE determines G(f).

Theoretical SLE: $V_\pi(f)$ is modelled as [11]

$$V_\pi(f) = V_{\pi 0} \cdot \frac{\alpha(f)L}{1 - e^{-\alpha(f)L}} \qquad (3)$$

Where $V_{\pi 0}$, α, and L denote V_π at DC, microwave loss factor and MZM electrode length, respectively. α(f) mainly depends on conductor loss α_c and dielectric loss α_d; for example, in LN MZM case [12]:

$$\alpha(f) = \alpha_c f^{1/2} + \alpha_d f \qquad (4)$$

Here, we study theoretical SLE of different MZMs assuming identical P_{LD} and R. In Fig. 1 we plot SLE in dB or 20*log10(SLE) (normalized to case (i) at *f*≈1kHz) of 4 MZMs that achieved >300Gb/s bit-rate:

(i) our high-SLE MZM ($V_{\pi 0}$=1.9V, l_C=3.3dB, l_P=0.5dB);

(ii) a thin-film LN (TFLN) MZM [4];

(iii) TFLN [4] but assuming a low l_C=3.3dB;

(iv) a SiPh MZM [5].

Although the 3dB BW is smaller, our MZM has a higher SLE at low frequencies, which yields competitive BER performance of optical&RF amplifier-free system, as shown next.

Theoretical SER/BER: Here we assume that fiber dispersion doesn't induce severe power fading and there's no optical or RF amplifier. In such case, we may use Gaussian approximation to derive theoretical SER. It needs the calculation of discrete-time channel impulse response (CIR) $\{g_n\}$. If the signal baud-rate is *B*, Tx & Rx use ideal low-pass filters (LPF, cut-off at *B*/2), Rx ideally samples at *B*, we have

$$g_n = \mathcal{F}^{-1}\left\{\underbrace{H(f)}_{LPF}\ \underbrace{\sqrt{G(f)}}_{MZM\,\&\,PD}\ Re\left[\underbrace{e^{j2\pi^2 f^2 \beta_2 L_F}}_{fiber}\right]\right\} \qquad (5)$$

Where $\mathcal{F}^{-1}$ and "Re" denote inverse discrete-time Fourier transform and taking real-valued part, respectively. For PAM-N format [13, 14],

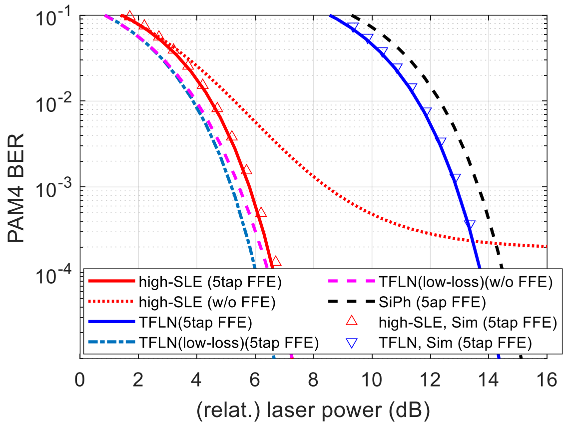

Fig. 2: Theoretical BERs and simulated BERs vs (relative) laser power of 150GBd PAM4 system with MZMs (i)~(iv). Optical back-to-back was assumed to emulate a fiber-dispersion-negligible regime. (The combined impact of dispersion is left for future work.)

$$SER_{PAM-N} = (N-1)/N \cdot \operatorname{erfc}\left(\sqrt{g_0^2 \Big/ \left[\frac{(N^2-1)}{3} \cdot \sum_{i\neq 0} g_i^2 + N_0\right]}\right) \qquad (6)$$

With Taylor expansion of Eq. (3)-(4) and approximations, one of approximated closed-form expression of $\{g_n\}$ could be:

$$g_0 \approx \frac{\pi P_{LD}}{V_{\pi 0} IL_{ff}}\left\{\frac{(L^2\alpha_c^2 - 3L\alpha_d)B}{8x} - \frac{L\alpha_c\sqrt{B}}{6\sqrt{2}} + \frac{1}{2}\right\} \qquad (7)$$

$$g_{\pm n} \approx \frac{\pi P_{LD}}{BV_{\pi 0} IL_{ff}}\left\{\begin{array}{c}\dfrac{A[\cos(n\pi) - 1]}{(2n\pi/B)^2} \\ +\dfrac{\sqrt{\pi}L\alpha_c \cdot S(\sqrt{2n})}{2\sqrt{2}(2n\pi/B)^{\frac{3}{2}}}\end{array}\right\} \qquad (8)$$

Where $A = (L^2\alpha_c^2 - 3L\alpha_d)/x$ (e.g., x=40) and $S(*)$ is the Fresnel Sine integral.

If finite-length digital FFE is considered, we first derive the FFE weight vector ***c*** using the orthogonality principle [14, 16], and total impulse response vector ***h*** is obtained by convolution:

$$\boldsymbol{h} = \boldsymbol{c} \otimes \boldsymbol{g} \qquad (9)$$

And [14, 15]

$$SER_{PAM-N} = (N-1)/N \cdot \operatorname{erfc}\left(\sqrt{h_0^2 \Big/ \left[\frac{(N^2-1)}{3} \cdot \sum_{i\neq 0} h_i^2 + N_0 \sum c_i^2\right]}\right) \qquad (10)$$

Finally, assuming 1 bit error per symbol error (e.g., by Gray coding), BER of PAM-N can be derived from SER as $BER = SER/\log_2 N$.

Fig. 2 shows the theoretical and simulated BER results of an 150GBd PAM4 (300Gb/s) IM-DD system with different MZMs (i)~(iv). When digital FFE is used, the theory can predict performance quite accurately without time-consuming Monte-Carlo simulations. Importantly, we can see that when digital FFE is used, our high-SLE MZM requires a relatively small laser

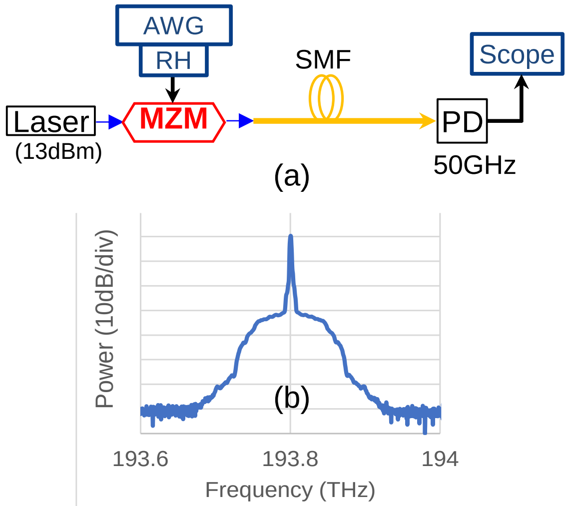

Fig. 3: (a) Experimental setup. RH: remote head. (b) Optical spectrum of 128GBd PAM8 signal at MZM output.

power, or equivalently, less demand for optical/RF amplification at the same BER level.

Experimental demonstration

The experimental setup is shown in Fig. 3(a). At the transmitter side, 128GBd electrical PAM8 signals were generated from a 256GS/s arbitrary waveform generator (AWG, Keysight M8199A) outputting at 2 samples per symbol (SpS) without any DSP, such that a high-resolution wideband DAC can be omitted. The peak-to-peak voltage (V_{pp}) of the signal was adjusted by a Keysight M8158A remote head. The signal was modulated onto a ≈100kHz-linewidth optical carrier at 193.8THz (≈1547nm) via our single-drive high-SLE MZM biased at the quadrature point. The prototype MZM has an insertion loss of 3.8dB, $V_{\pi 0}$ of 1.9V and ~5cm electrode length (with the same device structure as in ref. [17]). >6dBm Tx output was obtained with only 13dBm laser power; higher Tx output power is possible by using a power-tolerant polarizer at the input of the MZM waveguide. The optical double-sideband (DSB) PAM signal (optical spectrum shown in Fig. 3(b)) was then transmitted over 300m single-mode fiber (SMF, chromatic dispersion equivalent to >2km in O-band) to the receiver. The optical signal was detected by a 50GHz PD and captured by a 256GSa/s oscilloscope. The received optical power was 6dBm. The receiver did not involve optical or RF amplifier. The offline DSP includes resampling to 3-SpS and 10-tap LPF, down-sampling with synchronization, symbol-spaced DFE, and PAM8 demodulation.

Fig. 4(a) depicts the E/O response of the packaged MZM, showing a 6dB bandwidth of about 70GHz. The response at 50~100GHz would still be competitive to modulators with higher 3dB bandwidth but smaller SLE. Fig. 4(b) shows the BER vs. V_{pp} of 384Gb/s PAM8 after 300m SMF. Receiver-side DFE with 31 or 61 FF taps and 1 FB tap (denoted as DFE{31,1} and DFE{61,1}) was tested, and in the following measurements 900mV_{pp} was adopted. Fig. 4(c) shows the BER with number of FF taps in the DFE, both optical back-to-back (OBTB) and after 300m. BER better than 20% HD-FEC limit (BER of 1.44e-2 [18]) was achieved after 300m with DFE{41,1}; performance was improved with increased number of taps. Also, 20% soft-decision (SD)-FEC limit (BER of 2.4e-2 [19]) was reached with only DFE{13,1}. Finally, to show a higher data rate supported by the MZM, 140GBd (420Gb/s) root-raised-cosine (RRC)-shaped PAM8 after 300m was tested (V_{pp}=1.2V; using another 90GHz PD). BER<2.4e-2 was achieved with symbol-spaced 91-tap FFE.

Conclusions

We have demonstrated 384Gb/s PAM8 transmission over 300m in C-band with 900mV_{pp} driving voltages, optical & RF-amplifier-less reception, and low DSP complexity. A high-SLE MZM was fabricated and incorporated, while the theoretical background has been presented. Preliminary results of 140GBd (420Gb/s) PAM8 over 300m was also reported.

References

[1] M. S. B. Hossain, J. Wei, F. Pittalà, N. Stojanović, S. Calabrò, T. Rahman, G. Böcherer, T. Wettlin, C. Xie, M. Kuschnerov, and S. Pachnicke, "402 Gb/s PAM-8 IM/DD

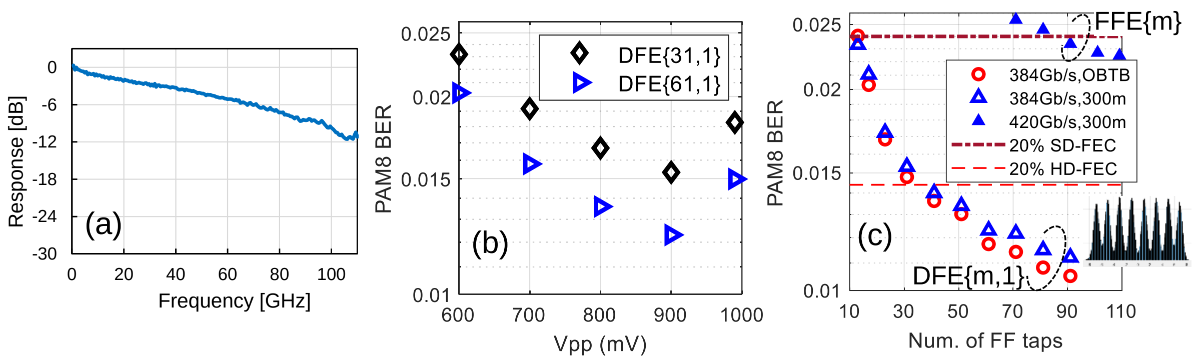

Fig. 4: Experimental results. (a) EO response of the prototype MZM. (b) BER vs. V_{pp} of 384Gb/s PAM8 signal after 300m SMF. "DFE{m,n}" denotes DFE with *m* FF and *n* FB taps. (c) BER vs. number of FF taps in DFE{m,1} (384Gb/s) or FFE{m} (420Gb/s); the inset shows a 384Gb/s PAM8 amplitude histogram after 300m SMF using DFE{91,1}.

O-Band EML transmission," Proc. ECOC 2021, We1C1.4.
[2] ETSI GS F5G 003 V1.1.1 (2021-09).
[3] C. Wang, M. Zhang, X. Chen, M. Bertrand, A. Shams-Ansari, S. Chandrasekhar, P. Winzer and M. Loncar, "Integrated lithium niobate electro-optic modulators operating at CMOS-compatible voltages," Nature, vol. 562, pp. 101-112, 2018.
[4] X. Chen, J. Cho, G. Raybon, D. Che, K.W. Kim, E. Burrows, P. Kharel, C. Reimer, K. Luke, L. He, and M. Zhang, "Single-wavelength and single-photodiode 700 Gb/s entropy-loaded PS-256-QAM and 200-GBaud PS-PAM-16 transmission over 10-km SMF," Proc. ECOC 2020, paper Th3A-2.
[5] M. S. Alam, X. Li, M. Jacques, E. Berikaa, P.-C. Koh, and D. V. Plant, "Net 300 Gbps/λ transmission over 2 km of SMF with a silicon photonic Mach-Zehnder modulator," IEEE PTL, vol. 33, no. 24, pp. 1391-1394, 2021.
[6] Q. Hu, R. Borkowski, Y. Lefevre, J. Cho, F. Buchali, R. Bonk, K. Schuh, E. De Leo, P. Habegger, M. Destraz, N. Del-Medico, H. Duran, V. Tedaldi, C. Funck, Y. Fedoryshyn, J. Leuthold, W. Heni, B. Baeuerle, and C. Hoessbacher, "Ultrahigh-net-bitrate 363 Gbit/s PAM-8 and 279 Gbit/s polybinary optical transmission using plasmonic Mach-Zehnder modulator," J. Lightwave Technol., vol. 40, no. 10, pp. 3338-3346, 2022.
[7] C. Eschenbaum, A. Mertens, C. Füllner, A. Kuzmin, A. Schwarzenberger, A. Kotz, G. Ramann, M. Chen, J. Drisko, B. Johnson, J. Zyskind, J. Marcelli, M. Lebby, W. Freude, S. Randel, and C. Koos, "Thermally stable Silicon-organic hybrid (SOH) Mach-Zehnder modulator for 140GBd PAM4 transmission with sub-1V drive signals," Proc. ECOC 2022, paper Th3B.2.
[8] R. Nagarajan, I. Lyubomirsky and O. Agazzi, "Low power DSP-based transceivers for data center optical fiber communications (Invited Tutorial)," J. Lightwave Technol., vol. 39, no. 16, pp. 5221-5231, 2021.
[9] Y. Lu and Y. Zhuang, "DSP and FEC considerations for 800GbE and 1.6TbE," www.ieee802.org/3/df/public/22_02/lu_3df_01b_220215.pdf.
[10] C. Cox III, E. I. Ackerman, G. E. Betts, and J. L. Prince, "Limits on the performance of RF-over-fiber links and their impact on device design," IEEE Trans. Microw. Theory & Tech., vol. 54, no. 2, pp. 906-920, 2006.
[11] Z. Liu and D. Zhu, "The effect of conductor loss on half-wave voltage and modulation bandwidth of electro-optic modulators," Chin. Opt. Lett., vol. 2, no. 10, pp. 586-589, 2004.
[12] Y. Yamaguchi, P. T. Dat, S. Takano, M. Motoya, S. Hirata, Y. Kataoka, J. Ichikawa, S. Oikawa, R. Shimizu, N. Yamamoto, K. Akahane, A. Kanno, and T. Kawanishi, "Traveling-wave Mach-Zehnder modulator integrated with electro-optic frequency-domain equalizer for broadband modulation," J. Lightwave Technol., DOI 10.1109/JLT.2023.3266988.
[13] A. Oppenheim and R. Schafer., Discrete-time signal processing (3rd ed.), Pearson, 2014.
[14] J. Weng and T. Le-Ngoc, "Performance Analysis of M-PAM Signalling with Tomlinson Harashima Precoding over ISI Channels," Proc. GlobeCom 2002, pp. 1-3.
[15] J. Proakis et al., Digital Communications.
[16] P. Zhu, Y. Yoshida, A. Kanno, and K. Kitayama, "Analysis and demonstration of low-complexity joint optical-electrical feedforward equalization (OE-FFE) for dispersion-limited high-speed IM/DD transmission," J. Lightwave Technol., vol. 41, no. 2, pp. 477-488, 2023.
[17] P. T. Dat, Y. Yamaguchi, M. Motoya, S. Oikawa, J. Ichikawa, A. Kanno, N. Yamamoto, and T. Kawanishi, "Transparent fiber–millimeter-wave–fiber system in 100-ghz band using optical modulator and photonic down-conversion," J. Lightwave Technol., vol. 40, no. 5, pp. 1483-1493, 2022.
[18] L. M. Zhang and F. Kschischang, "Staircase codes With 6% to 33% overhead," J. Lightwave Technol., vol. 32, no. 10, pp. 1999-2002, 2014.
[19] D. Chang, F. Yu, Z. Xiao, Y. Li, N. Stojanovic, C. Xie, X. Shi, X. Xu, and Q. Xiong, "FPGA verification of a single QC-LDPC code for 100 Gb/s optical systems without error floor down to BER of 10^{-15}," Proc. OFC 2011, paper OTuN.2.